5540 *Biochemistry* **2010,** *49,* 5540–5552
DOI: 10.1021/bi100071j

BIOCHEMISTRY
including biophysical chemistry & molecular biology
Article

Probing the Recognition Surface of a DNA Triplex: Binding Studies with Intercalator−Neomycin Conjugates[†]

Liang Xue,[‡] Hongjuan Xi, Sunil Kumar, David Gray, Erik Davis, Paris Hamilton, Michael Skriba, and Dev P. Arya*

Laboratory of Medicinal Chemistry, Department of Chemistry, Clemson University, Clemson, South Carolina 29634 [‡]*Present address: Department of Chemistry, University of the Pacific, Stockton, CA 95211.*

Received January 15, 2010; Revised Manuscript Received May 14, 2010

ABSTRACT: Thermodynamic studies on the interactions between intercalator−neomycin conjugates and a DNA polynucleotide triplex [poly(dA)·2poly(dT)] were conducted. To draw a complete picture of such interactions, naphthalene diimide−neomycin (**3**) and anthraquinone−neomycin (**4**) conjugates were synthesized and used together with two other analogues, previously synthesized pyrene−neomycin (**1**) and BQQ−neomycin (**2**) conjugates, in our investigations. A combination of experiments, including UV denaturation, circular dichroism (CD) titration, differential scanning calorimetry (DSC), and isothermal titration calorimetry (ITC), revealed that all four conjugates (**1**−**4**) stabilized poly(dA)·2poly(dT) much more than its parent compound, neomycin. UV melting experiments clearly showed that the temperature ($T_{m3\rightarrow2}$) at which poly(dA)·2poly(dT) dissociated into poly(dA)·poly(dT) and poly(dT) increased dramatically (>12 °C) in the presence of intercalator−neomycin conjugates (**1**−**4**) even at a very low concentration (2 μM). In contrast to intercalator−neomycin conjugates, the increment of $T_{m3\rightarrow2}$ of poly(dA)·2poly(dT) induced by neomycin was negligible under the same conditions. The binding preference of intercalator−neomycin conjugates (**1**−**4**) to poly(dA)·2poly(dT) was also confirmed by competition dialysis and a fluorescent intercalator displacement assay. Circular dichroism titration studies revealed that compounds **1**−**4** had slightly larger binding site size (∼7−7.5) with poly(dA)·2poly(dT) as compared to neomycin (∼6.5). The thermodynamic parameters of these intercalator−neomycin conjugates with poly(dA)·2poly(dT) were derived from an integrated van't Hoff equation using the $T_{m3\rightarrow2}$ values, the binding site size numbers, and other parameters obtained from DSC and ITC. The binding affinity of all tested ligands with poly(dA)·2poly(dT) increased in the following order: neomycin < **1** < **3** < **4** < **2**. Among them, the binding constant [$(2.7 \pm 0.3) \times 10^8$ M^{-1}] of **2** with poly(dA)·2poly(dT) was the highest, almost 1000-fold greater than that of neomycin. The binding of compounds **1**−**4** with poly(dA)·2poly(dT) was mostly enthalpy-driven and gave negative ΔC_p values. The results described here suggest that the binding affinity of intercalator−neomycin conjugates for poly(dA)·2poly(dT) increases as a function of the surface area of the intercalator moiety.

Targeting the major groove of the DNA duplex with a single-stranded DNA to produce a DNA triple-helical structure has aroused much interest, especially in the past two decades, since its discovery in the 1950s (*1*). Such recognition obeys well-defined base pairing rules by making specific hydrogen bond contacts between nucleobases of the third strand and substituents on the exposed faces of the Watson−Crick base pairs, known as the purine and pyrimidine motifs, which have been examined by many investigators (*2*−*6*). DNA triple-helical structures formed in vivo under physiological conditions have been observed and named "H-DNA", yet much remains to be learned about their biological functions (*7*, *8*). A well-designed synthetic DNA oligonucleotide [also known as triplex-forming oligonucleotide (TFO)][1] binds to DNA duplex in a sequence-specific manner. Evidence suggesting that TFOs can effectively block the binding of a variety of proteins to DNA duplexes raises the level of importance of their potential therapeutical uses. Examples of triplex formation that inhibit cleavage of DNA mediated by topoiosomerase II and interfere with the unwinding function of DNA helicases are well-documented (*9*, *10*). Several groups have revealed inhibition of transcription by blockage of DNA or RNA polymerase using the triplex strategy in the promoter (P1) of the *c-myc* oncogene (*11*, *12*) and in the α subunit of the interleukin-2 receptor (IL-2Rα) (*13*, *14*).

In spite of its promising sequence-specific recognition of DNA duplex, the triplex formation strategy, also known as Antigene, has some limitations (*3*, *15*). A DNA triplex is more difficult to form than a DNA duplex because of the electrostatic repulsions between the negatively charged backbone(s) of TFO and the DNA duplex. In addition, the formation of the DNA triplex is energetically less favorable, and the resulting DNA triplex is less stable than its counterpart duplex.

Over the years, several strategies for overcoming the instability of the DNA triplex, such as modification of nucleobases and backbone groups of TFO (*16*−*18*) and utilization of small binding molecules (*19*−*22*), have been investigated. Interestingly, many DNA duplex intercalators have been found to stabilize DNA triple-helical structures, although the selectivity of these molecules between the DNA triplex and duplex is

[†]We are grateful for support of this research by the National Science Foundation (CHE/MCB-0134972) and the National Institutes of Health (R15CA125724).

*To whom correspondence should be addressed. E-mail: dparya@clemson.edu. Phone: (864) 656-1106. Fax: (864) 656-6613.

[1]Abbreviations: FID, fluoroscent intercalator displacement; TFO, triplex-forming oligonucleotide; BQQ, benzoquinoquinoxaline.

 Published on Web 05/25/2010

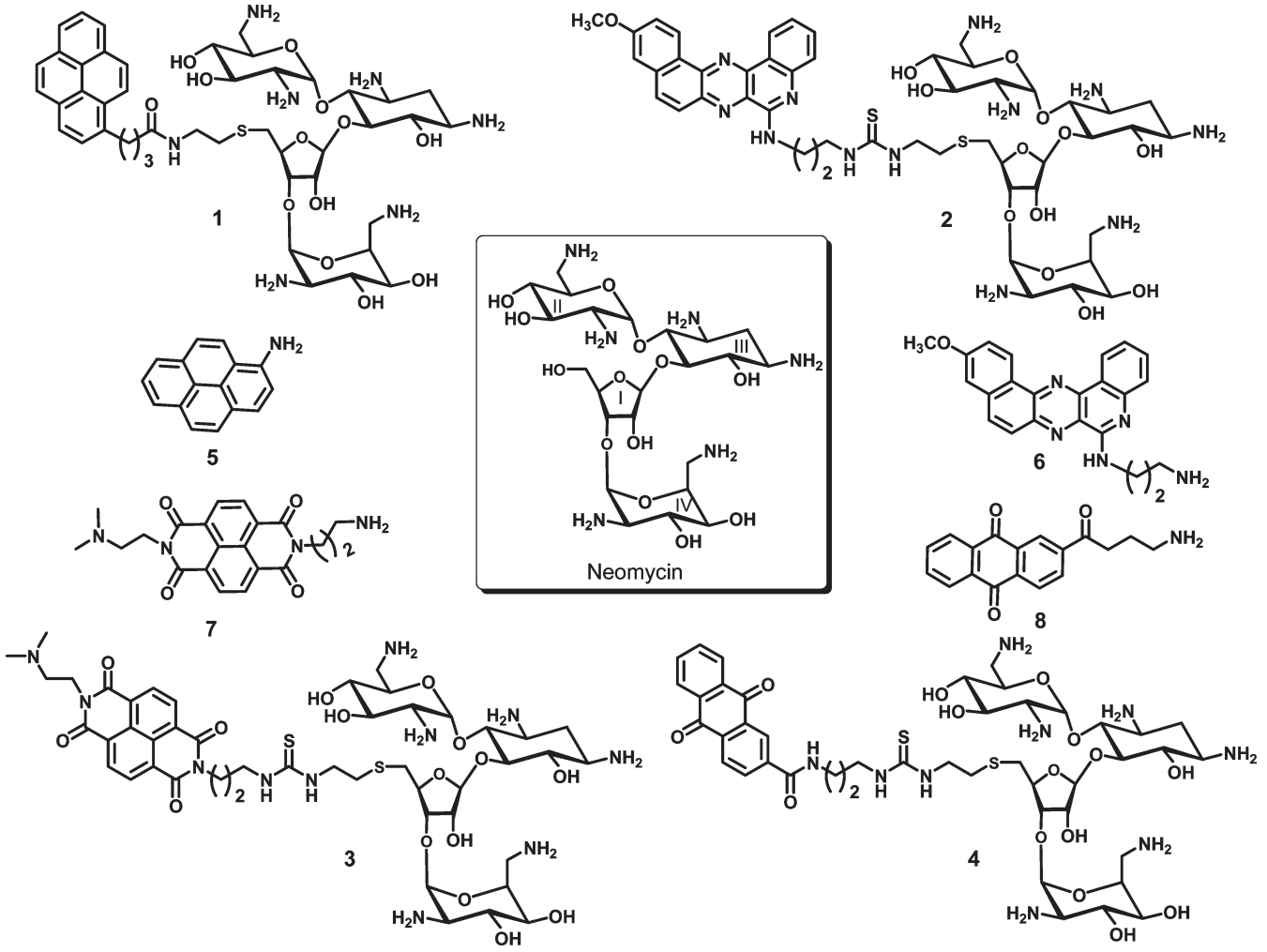

FIGURE 1: Structures of neomycin and intercalator−neomycin conjugates.

subtle (*23*). Helene and co-workers rationally designed and synthesized benzopyridoindole derivatives, which prefer to bind the DNA triplex over the duplex and increase the rate of triplex formation (*24*, *25*). We have reported the discovery of the first DNA triplex-specific groove binder, neomycin [an antibiotic (Figure 1)] (*26*, *27*). Our results showed that among all the aminoglycosides, neomycin specifically stabilizes DNA triple-helical structures such as poly(dA)·2poly(dT), AT-rich or mixed base of DNA oligonucleotide triplexes, and a 12-mer intramolecular DNA triplex while having a weaker effect or no effect on DNA duplexes (*26*). Furthermore, modeling studies of a system including neomycin and a $(dT)_{10}\cdot(dA)_{10}\cdot(dT)_{10}$ DNA triplex suggest that neomycin most likely binds in the Watson−Hoogsteen groove of the DNA triplex with its ring I sitting in the center of the groove and rings II and IV bridging the two pyrimidine strands together (*27*). These reports expanded the number of nucleic acids that aminoglycosides have been shown to bind and suggested that the aminoglycoside preference is for smaller A-form major grooves (*28*−*43*). Further expanding the family of DNA triplex binding ligands based on the structure of neomycin was achieved by conjugating intercalators such as pyrene and BQQ with neomycin to yield pyrene−neomycin (**1**) and BQQ−neomycin (**2**) conjugates (Figure 1). UV denaturation and circular dichroism studies of DNA triplexes with **1** and **2** reveal that these two conjugates enhance the stabilization of DNA triplexes much more than their parent compound, neomycin (*44*, *45*). In addition, covalent attachment of intercalators to neomycin seems not to alter the selective binding of neomycin to the DNA triplex over the duplex. The observed enhancement of DNA triplex stabilization by **1** and **2** is attributed to the "dual recognition mode", in which the neomycin moiety binds in the Watson−Hoogsteen groove when the intercalator inserts between the proximate base triplets to provide additional stabilization.

Further understanding of interactions of intercalator−neomycin conjugates with DNA triplexes can be achieved by acquiring thermodynamic parameters of their binding events. For a complete study, we in this period have synthesized two additional intercalator−neomycin conjugates, naphthalene diimide−neomycin (**3**) and anthraquinone−neomycin (**4**). We probe the surface area of the DNA triplex using compounds **1**−**4** with varying surfaces for stacking between the DNA triplets (Figure 1). Fluorescent intercalator displacement (FID) assays were first performed to estimate the relative affinities of these ligands for the DNA triplex. The binding enthalpies, entropies, and equilibrium constants of these intercalator−neomycin conjugates (**1**−**4**) with a DNA polynucleotide triplex, poly(dA)·2poly(dT) were derived from an integrated van't Hoff equation (*46*) to exploit the effect of the intercalator moiety and the important factors on the stabilization of the DNA triplex.

EXPERIMENTAL PROCEDURES

General Methods. Unless otherwise specified, chemicals were purchased from Aldrich (St. Louis, MO) or Fisher Scientific (Pittsburgh, PA) and used without further purification.

Neomycin sulfate was purchased from ICN Biomedicals (Solon, OH) and was used without further purification. Mini-dialysis flotation devices were acquired from Pierce (Rockford, IL). Polynucleotides were purchased from GE Healthcare (Piscataway, NJ). The concentrations of the polynucleotide solutions were determined by UV spectroscopy, using the following molar extinction coefficients: ε_{264} = 8520 M^{-1} cm^{-1} $base^{-1}$ for poly(dT), and ε_{260} = 6000 M^{-1} cm^{-1} bp^{-1} for poly(dA)·poly(dT). Oligonucleotides were synthesized and purified by IDT (Coralville, IA). ^{1}H NMR spectra were recorded on a JEOL (Tokyo, Japan) ECA 500 MHz FT-NMR spectrometer. MS (MALDI-TOF) spectra were recorded using a Kratos (Columbia, MD) analytical KOMPACT SEQ mass spectrometer. UV spectra were recorded on a Varian (Walnut Creek, CA) Cary 1E UV−vis spectrophotometer. FID assays were conducted using a Photon Technology International (Lawrenceville, NJ) instrument. Isothermal titration calorimetric measurements were performed on a MicroCal (Piscataway, NJ) VP-ITC isothermal titration calorimeter. Circular dichroism spectra were recorded on a JASCO (Easton, MD) J-810 spectropolarimeter equipped with a thermoelectrically controlled cell holder. Differential scanning calorimetric measurements were taken on a MicroCal VP-DSC differential scanning calorimeter.

(*i*) *Preparation of* ***3a***. To an anhydrous pyridine solution (2 mL) of compound **12** (18 mg, 0.014 mmol) were added compound **5** (7.6 mg, 0.015 mmol) and DMAP (catalytic amount). After the mixture had been stirred under N_2 at room temperature overnight, the organic solvent was removed under vacuum. Flash chromatography of the residue (6% MeOH in CH_2Cl_2) yielded the desired product as a white solid (15 mg, 86%): R_f = 0.33 (silica gel, 6% MeOH in CH_2Cl_2); ^{1}H NMR (CD_3OD) δ 8.74−8.77 (m, 4H), 5.40 (br, 1H), 5.37 (m, 1H), 5.11 (m, 1H), 4.90 (m, 1H), 4.23 (m, 1H), 4.09 (m, 2H), 3.82 (m, 4H), 3.76 (m, 2H), 3.67 (m, 2H), 3.44−3.56 (m, 6H), 3.00−3.30 (m, 9H), 2.84−2.86 (m, 4H), 2.70−2.78 (m, 6H), 2.69 (m, 4H), 2.35 (m, 6H), 2.03 (m, 2H), 1.94 (m, 1H), 1.40 (m, 54H); MS (MALDI-TOF) calcd for $C_{77}H_{119}N_{11}O_{28}S_2$ 1610.96, found 1611.56.

(*ii*) *Preparation of* ***3***. In a 10 mL round-bottom flask, **3a** (15 mg, 0.090 mmol) was dissolved in a 1:1 TFA/CH_2Cl_2 mixture (2 mL) and the solution stirred at room temperature for 3 h. The solvent was removed under vacuum, and the residue was dissolved in deionized water (20 mL). The aqueous layer was washed with ether (3 × 20 mL). Lyophilization yielded **3** as a yellow solid (9 mg, 90%): ^{1}H NMR (CD_3OD) δ 8.74−8.77 (m, 4H), 5.40 (br, 1H), 5.37 (m, 1H), 5.11 (m, 1H), 4.90 (m, 1H), 4.90 (q, 2H) 4.23 (m, 2H), 4.09 (m, 2H), 3.82 (m, 6H), 3.76 (m, 6H), 3.67 (m, 2H), 3.44−3.56 (m, 6H), 3.00−3.30 (m, 12H), 2.84−2.86 (m, 6H), 2.70−2.78 (m, 8H), 2.69 (m, 4H), 2.45 (m, 2H), 2.03 (m, 2H), 1.94 (m, 1H), 1.45 (m, 2H).

(*iii*) *Preparation of* ***4a***. To an anhydrous pyridine solution (5 mL) of compound **12** (10.7 mg, 0.008 mmol) were added compound **6** (9.3 mg, 0.027 mmol) and DMAP (catalytic amount). After the mixture had been stirred at room temperature overnight, the organic solvent was removed under vacuum. Flash chromatography of the residue (5% MeOH in CH_2Cl_2) yielded the desired product as a white solid (7.1 mg, 86%): R_f = 0.60 (silica gel, 10% MeOH in CH_2Cl_2); ^{1}H NMR (CD_3OD) δ 8.60 (s, 1H), 8.20−8.40 (br, 1H), 5.37 (m, 1H), 5.11 (m, 1H), 4.90 (m, 1H), 4.23 (m, 1H), 4.09 (m, 2H), 3.82 (m, 4H), 3.76 (m, 2H), 3.67 (m, 2H), 3.44−3.56 (m, 6H), 3.00−3.30 (m, 9H), 2.84−2.86 (m, 4H), 2.70−2.78 (m, 6H), 2.69 (m, 4H), 2.35 (m, 6H), 2.03 (m, 2H), 1.94 (m, 1H), 1.40 (m, 54H); MS (MALDI-TOF) calcd for $C_{74}H_{113}N_9O_{27}S_2Na^+$ $(M + Na)^+$ 1646.86, found 1647.19.

(*iv*) *Preparation of* ***4***. In a 10 mL round-bottom flask, **4a** (7.1 mg, 0.090 mmol) was dissolved in a 1:1 TFA/CH_2Cl_2 mixture (2 mL) and the solution stirred at room temperature for 3 h. The solvent was removed under vacuum, and the residue was dissolved in deionized water (20 mL). The aqueous layer was washed with ether (3 × 20 mL). Lyophilization yielded **3** as a yellow solid (9 mg, 90%): ^{1}H NMR (CD_3OD) δ 8.60 (s, 1H), 8.20−8.40 (m, 4H), 7.8−7.84 (m, 2H), 5.40 (br, 1H), 5.37 (m, 1H), 5.11 (m, 1H), 4.90 (m, 1H), 4.50 (m, 2H), 4.23 (m, 1H), 4.09 (m, 2H), 3.82 (m, 4H), 3.76 (m, 2H), 3.67 (m, 2H), 3.44−3.56 (m, 8H), 3.00−3.30 (m, 10H), 2.84−2.86 (m, 4H), 2.70−2.78 (m, 6H), 2.69 (m, 4H), 2.35 (m, 6H), 2.03 (m, 2H), 1.94 (m, 1H); MS (MALDI-TOF) calcd for $C_{44}H_{65}N_9O_{15}S_2Na^+$ $(M + Na)^+$ 1047.2, found 1046.9.

Preparation of Poly(dA)·2Poly(dT). The poly(dA)·poly(dT) duplex (100 μM/triplet) and poly(dT) (100 μM/triplet) were dissolved in a mixture (1.5 mL) of sodium cacodylate (SC, 10 mM, pH 6.8), KCl (150 mM), and EDTA (0.5 mM). The mixture was heated at 90 °C for 10 min, slowly cooled to room temperature, and incubated at 4 °C for 12 h to maximize the extent of DNA triplex formation.

Isothermal Titration Calorimetry (ITC). Into a mixture (1.42 mL) of a poly(dA)·2poly(dT) DNA solution (100 μM), sodium cacodylate (10 mM, pH 6.8), KCl (150 mM), and EDTA (0.5 mM) in a sample cell at 20 °C was constantly injected an aliquot of a mixture (10 μL) of the ligand of interest (1−200 μM), sodium cacodylate (10 mM, pH 6.8), KCl (150 mM), and EDTA (0.5 mM) through a rotary syringe. The interval between each injection was 300 s, and the duration of each injection was 20 s. The syringe rotated at 260 rpm. The calorimetric spectrum was recorded after each injection and was processed using Origin version 5.0. The spectra obtained from injection of the ligand solution at the same concentration into a buffer solution [10 mM sodium cacodylate, 150 mM KCl, and 0.5 mM EDTA (pH 6.8)] at 20 °C were used as blanks. Integration of the area under each heat burst curve yielded the heat given off upon each injection.

To calculate the actual heat produced from binding of ligand to DNA triplex, the following equation was used.

$$\Delta H_{\text{actual}} = \Delta H_{\text{measured}} - \Delta H_{\text{blank}}$$

where ΔH_{actual} is the actual heat produced by the binding of ligand to the DNA triplex, $\Delta H_{\text{measured}}$ is the measured heat from the titration curve, and ΔH_{blank} is the heat produced from injection of ligand into the buffer solution (blank).

UV Denaturation. The UV denaturation samples (1 mL) were prepared by mixing the poly(dA)·2poly(dT) DNA (15 μM/triplet), sodium cacodylate (10 mM, pH 6.8), KCl (150 mM), EDTA (0.5 mM), and one of the intercalator−neomycin conjugates (**1**−**4**) at various concentrations (0, 1, 2, 4, 10, 15, and 25 μM). The UV melting spectra of these samples in 1 cm path length quartz cuvettes were recorded at 260 and 280 nm as a function of temperature (5−95 °C, heating rate of 0.2 °C/min). The melting temperature was determined as the one that has the peak value in the first derivative of the melting curve.

Circular Dichroism (CD) Titration Measurements. Into a mixture (1.8 mL) of a poly(dA)·2poly(dT) DNA solution (50 μM/base triplet), sodium cacodylate (10 mM, pH 6.8), KCl (150 mM), and EDTA (0.5 mM) in a 1 cm path length quartz

Scheme 1 [a]

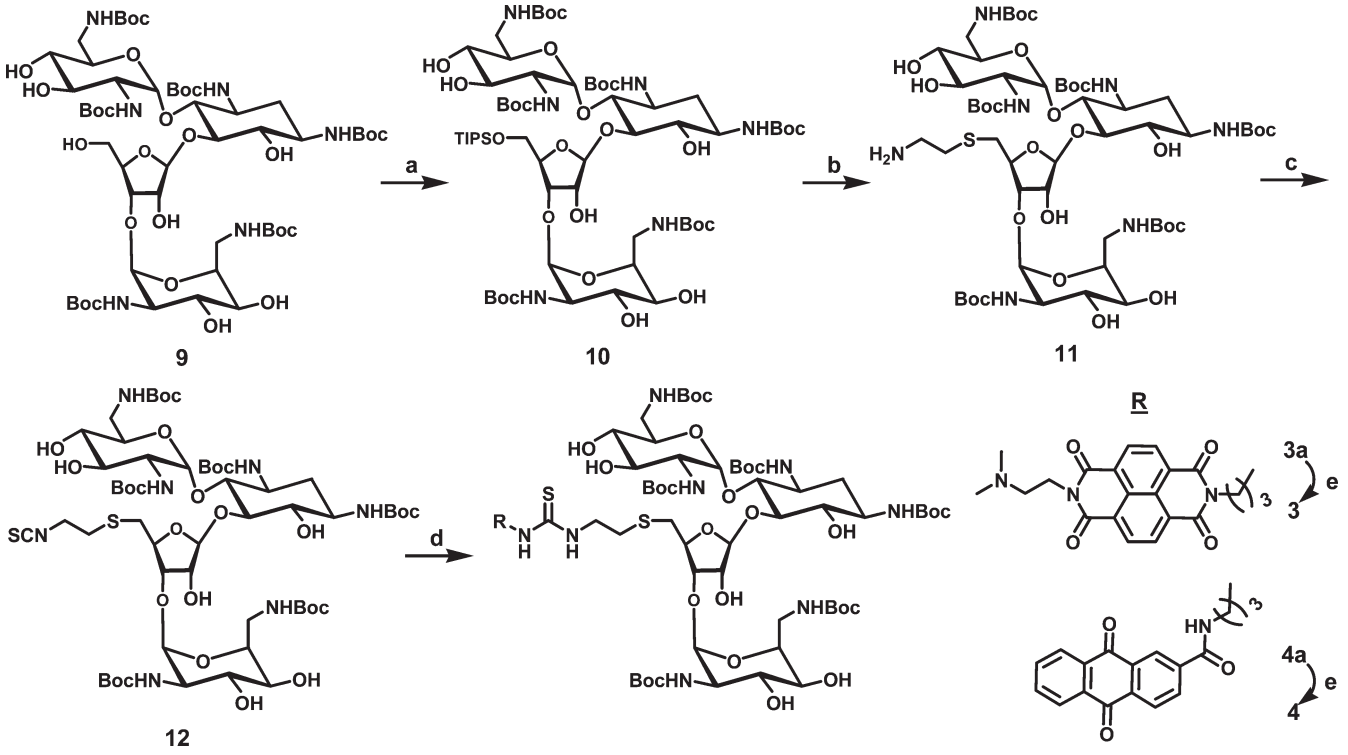

[a] (a) 2,4,6-Triisopropylbenzenesulfonlyl chloride, pyridine, room temperature; (b) 1,2-aminothiolethane, Na, EtOH; (c) TCDP, DCM, room temperature; (d) **7** or **8**, CH_2Cl_2; (e) TFA/CH_2Cl_2.

cuvette at 20 °C were injected aliquots (0.6−40 μL) of the intercalator−neomycin stock aqueous solution. The solution was then mixed by gentle inversion of the close capped cuvette several times. The interval between each injection was 10 min. The circular dichroism spectra were recorded as a function of wavelength (200−350 nm).

Competition Dialysis Measurements. Nucleic acid solutions were prepared in phosphate buffer (8 mM, pH 7.0) and NaCl (185 mM) to yield a final concentration of 75 μM (per monomeirc unit of each polymer). The nucleic acid solution (200 μL) was placed into a mini-dialysis unit and then allowed to equilibrate against a phosphate buffer (400 mL) of ligand (1 μM) at room temperature for 72 h. At the end of the experiment, nucleic acid samples (180 μL) were carefully removed and were taken to a final concentration of sodium dodecyl sulfate [SDS, 1% (w/v)]. After equilibration for 2 h, the concentration of ligand was determined spectroscopically. An appropriate correction was made due to volume changes.

The following nucleic acids (*47*) were used in the experiments: 16S A-site rRNA, i-motif, poly(dA)·poly(rU), poly(rA)·poly(dT), poly(dG)·poly(rC), poly(dA-dT), *Clostridium perfringens* DNA, *Micrococcus lysodeikticus* DNA, calf thymus DNA, poly(dA)·2poly(dT), poly(dA)·poly(dT), poly(dA), poly(dT), poly(rA)·2poly(rU), poly(rA)·poly(rU), poly(rA), and poly(rU).

Fluorescence Intercalator Displacement Assay (*FID*). Thiazole orange (700 nM) was dissolved in a buffer solution [10 mM sodium cacodylate, 150 mM KCl, and 0.5 mM EDTA (pH 6.8 or 5.5)], and its fluorescence was recorded (excitation at 504 nm, emission at 520−600 nm). The triplex deoxynucleotide hairpin 5′-dA_{12}-x-dT_{12}-x-dT_{12}-3′ (where x is hexaethylene glycol) was added to the thiazole orange solution to yield a final DNA concentration of 100 nM (per strand), and the fluorescence was measured again and normalized to 100% relative fluorescence. A concentrated solution of compound (100 μM to 10 mM) was added, and the fluorescence was measured after incubation at 10 °C for 5 min. The addition of compound was continued until the fluorescence reached saturation. For all titrations, final concentrations were corrected for dilution (< 5% of the total volume).

For the FID assay using the plate reader, the procedures were as follows. The solution of poly(dA)·2poly(dT) was incubated with thiazole orange for 30 min prior to use for FID titration. Each well of a 96-well plate was loaded with a poly(dA)·2poly(dT) solution (200 μL each). A concentrated solution of ligand (**1**−**8**) (9.35−935 μM) was added, and the fluorescence was measured after incubation for 5 min. The 96-well plate was read in triplicate on a Cary eclipse plate reader fluorometer with advanced reads software (excitation at 504 nm, emission at 532 nm, 430−1100 nm cutoff filter) (no ligand, 100% fluorescence; no DNA, 0% fluorescence). Fluorescence readings are reported as percent fluorescence relative to control wells.

RESULTS AND DISCUSSION

Synthesis of Naphthalene diimide−Neomycin and Anthraquinone−Neomycin Conjugates. We recently prepared two intercalator−neomycin conjugates (**1** and **2**) by tethering the intercalator moiety at the 5′-OH position of neomycin (*44*, *45*). The synthesis of **3** and **4** in the study presented here adopted the same synthetic strategy, in which the 5′-OH position of neomycin was selected to tether the intercalators because of the ease of modification at this position (*45*, *48*, *49*). Typically, reaction of t-Boc-protected neomycin with 2,4,6-triisopropylbenzenesulfonlyl chloride was followed by treatment of 1,2-aminothiolethane to yield compound **11** (Scheme 1). The amino group of **11** was further converted into an isothiocyanate group by reaction with

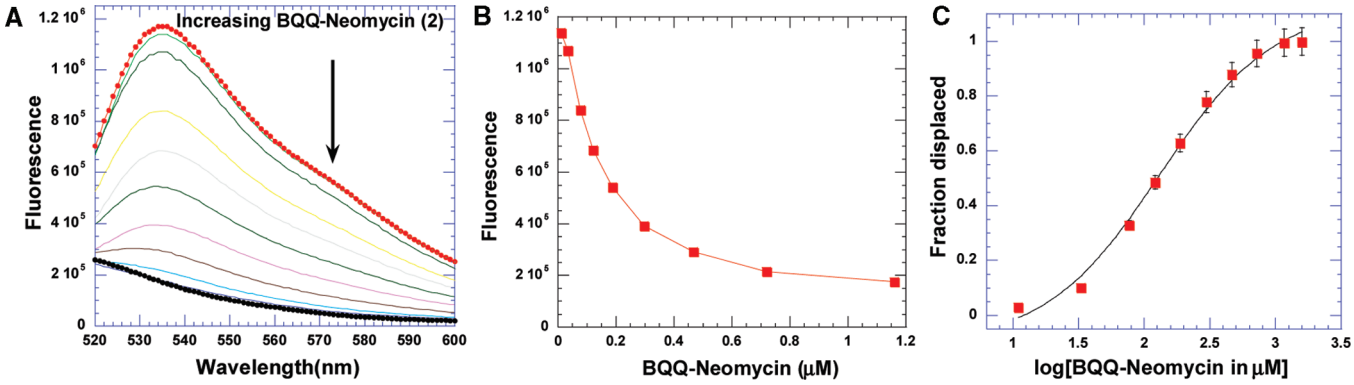

FIGURE 2: Graphical representation of the thiazole orange displacement assay. (A) Raw emission data of 1.25 μM thiazole orange upon excitation at 534 nm with buffer only (○) and after addition of 0.88 μM poly(dA)·2poly(dT) triplex (●). The BQQ−neomycin conjugate was then titrated from 0.25 μM to 1.06 mM. (B) Decrease in the fluorescence intensity of the complex (DNA−thiazole orange) upon addition of aliquots of the BQQ−neomycin conjugate. (C) Assuming a linear relationship between the changes in fluorescence intensity with the fraction of thiazole orange displaced results in an S-shaped binding isotherm. This graph allows determination of the concentration of ligands needed to displace half of the thiazole orange from the DNA triplex. Buffer conditions: 150 mM KCl, 10 mM SC, 0.5 mM EDTA, pH 6.8, 0.88 μM poly(dA)·2poly(dT)/base triplet, 1.25 μM TO.

1,1′-thiocarbonyldi-2-(1*H*)-pyridone (TCDP) to yield **12** (*37*). Subsequently reacting **12** with an intercalator (**7** or **8**) yielded **3a** or **4a**, with a thiourea linkage in decent yields. Treatment of **3a** and **4a** with trifluoroacetic acid (TFA) removed the acid labile Boc-protecting groups to produce **3** and **4**, respectively, in quantitative yields. It is noteworthy that compound **12** has broad applications in terms of conjugation of neomycin with other moieties containing amino groups (Scheme 1) (*37*, *50*).

FID Assay as a Rapid Probe for Conjugate Affinities. The fluorescence intercalator displacement (FID) method, a technique complementing the limitations of ITC in calculating the intrinsic affinities, has been introduced by Boger (*51*). In this method, an intercalator such as ethidium bromide (EB) or thiazole orange (TO) intercalates into a DNA triplex to form a complex solution. The bound intercalator fluoresces more significantly than the free intercalator. Titration of a competitive ligand that has a high binding affinity for the DNA triplex into the solution will in principle displace the bound intercalator. The amount of displaced bound intercalator can be measured as a function of the decrease in fluorescence; ethidium bromide, which intercalates into nucleic acids with a moderate affinity (*51*), is known to be displaced by a competitive ligand. Thiazole orange was used in our assay because it gave much greater fluorescence enhancement (3000-fold increment) upon intercalation into DNA than ethidium bromide (20-fold increment) (*52*).

The displacement assays were first performed as complete titrations on a fluorometer (Figure 2) and were then run (in triplicate) on a 96-well plate reader at a salt concentration of 150 mM KCl (Figure 1a−c). The polynucleotide triplex poly(dA)·2poly(dT) and a smaller intramolecular triplex hairpin 5′-dA$_{12}$-x-dT$_{12}$-x-dT$_{12}$-3′ were used to assess the affinities of the conjugates. The AC$_{50}$ values reported in Table 1 represent the ligand concentrations required to displace 50% of thiazole orange from the triplex, as measured by a 50% reduction of the initial bound thizaole orange fluorescence. The AC$_{50}$ values for different intercalators and intercalator−neomycin conjugates are listed in Table 1. **2** has the lowest AC$_{50}$ value among all the intercalator−neomycin conjugates, suggesting that it binds to the DNA triplex more tightly than other conjugates. The rank order for binding to poly(dA)·2poly(dT) given by the AC$_{50}$ values is as follows: neomycin (3 μM) < **3** (1.56 μM) < **1** (366 nM) < **4** (138 nM) < **2** (124 nM). A similar trend in binding affinity was observed in the experiments with the 5′-dA$_{12}$-x-dT$_{12}$-x-dT$_{12}$-3′ triplex. The AC$_{50}$ of neomycin (47.4 μM) is approximately 100-fold higher than that of **2** (379 nM) and approximately 50-fold higher than that of **4** (713 nM). Surprisingly, the AC$_{50}$ value of **1** is smaller than that of **3** even though **3** has a larger surface area for interaction with DNA than **1**. It is noteworthy that the trend of AC$_{50}$ values for intercalators follows the same pattern observed for intercalator−neomcyin conjugates. In particular, the rationally designed triplex-specific ligand BQQ has the lowest AC$_{50}$ value, indicating the highest affinity for the DNA triplex among the tested intercalators. When the FID experiments were conducted with the poly(dA)·poly(dT) duplex, thiazole orange could not be displaced by 10 mM neomycin, suggesting that the affinity of the aminoglycoside is 2−3 orders of magnitude lower for the AT-rich DNA duplex than for the AT-rich DNA triplex.

Table 1: AC$_{50}$ Values for Binding of Various Neomycin Conjugates to the DNA Triplex[a]

aminoglycoside conjugate	AC$_{50}$ (5′-dA$_{12}$-x-dT$_{12}$-x-dT$_{12}$-3′)	AC$_{50}$ [poly(dA)·2poly(dT)]
6		1.59 ± 0.04 μM
8		4.4 ± 0.7 μM
7		7.2 ± 0.9 μM
2	379 ± 86 nM	124 ± 18 nM
4	713 ± 123 nM	138 ± 20 nM
1	1.78 ± 0.32 μM	366 ± 13 nM
3	5.37 ± 1.46 μM	1.56 ± 0.29 μM
neomycin	47.4 ± 2.1 μM	3.0 ± 0.6 μM

[a]Buffer conditions: 150 mM KCl, 10 mM SC, 0.5 mM EDTA, and 100 nM 5′-dA$_{12}$-x-dT$_{12}$-x-dT$_{12}$-3′/strand with 700 nM TO or 0.88 μM poly(dA)·2poly(dT)/base triplet with 1.25 μM TO.

UV Denaturation of Poly(dA)·2Poly(dT) with Intercalator−Neomycin Conjugates. The thermal stability of DNA triple-helical structures can be examined using UV denaturation. Biphasic transitions are commonly observed when the UV spectrum of the DNA triplex is monitored as a function of temperature, which represents dissociation of the DNA triplex into its counterpart duplex at lower temperatures and further dissociation of the resulting DNA duplex into single-stranded structures at higher temperatures. Measuring the melting temperatures of the DNA triplex in the presence of binding ligands is

Table 2: UV Melting Temperatures Recorded When Poly(dA)·2Poly(dT) Dissociated in the Presence of Intercalator−Neomycin Conjugates (**1**−**4**) at Various Concentrations[a]

concentration (μM)	$T_{m3\rightarrow2}$	$T_{m2\rightarrow1}$
	1	
0	34	72
1	43	72
2	56	72
4	59	73
	2	
0	34	72
2	80 ($T_{m3\rightarrow1}$)	−
4	86 ($T_{m3\rightarrow1}$)	−
	3	
0	34	72
1	54	72
2	65	73
4	70	75
	4	
0	34	72
1	60	74
2	68	74
4	74	80

[a] $T_{m3\rightarrow2}$ is thehe melting temperature representing the dissociation of poly(dA)·2poly(dT) to poly(dA)·poly(dT) and poly(dT). $T_{m2\rightarrow1}$ is the melting temperatures representing the dissociation of poly(dA)·poly(dT) to poly(dA) and poly(dT).

a quick and unambiguous way to simultaneously determine the relative strength of ligands on stabilization of the DNA triplex and the selectivity of ligands between the DNA triplex and duplex. A DNA polynucleotide triplex such as poly(dA)·2poly(dT) was used as a model DNA triplex in UV denaturation because of its clear transitions of triplex into duplex and duplex into random coil structures. Under our experimental conditions, in the absence of ligands, the melting temperatures of poly(dA)·2poly(dT) dissociating into poly(dA)·poly(dT) and poly(dT) and poly(dA)·poly(dT) dissociating into poly(dA) and poly(dT) were 34 and 72 °C, respectively. Our UV denaturation results suggested that all four intercalator−neomycin conjugates dramatically stabilized poly(dA)·2poly(dT) and had little effect on its duplex, poly(dA)·poly(dT) (Table 2). Among the four, compound **2** exhibited the greatest stabilization on poly(dA)·2poly(dT). In the presence of **2** (4 μM), only one melting transition at 86 °C was observed (Figure 1 of the Supporting Information), indicating the merging of triplex to duplex and duplex to single-strand transitions (*53*). In contrast, the UV melting temperatures representing the triplex to duplex transition in the presence of neomycin, **1**, **3**, and **4** at the same concentration (4 μM) were 40, 58, 70, and 74 °C, respectively (Table 2). In all cases, the changes in DNA duplex melting temperature were subtle. The stabilization of poly(dA)·2poly(dT) seems to result from the covalent attachement of the intercalator and neomycin since a mixture of intercalator and neomycin does not show the equivalent stabilization. For instance, the melting temperature of poly(dA)·2poly(dT) in the presence of **7** (4 μM) and neomycin (4 μM) was 50 °C, ~20 °C lower than that in the presence of **3** at the same concentration (4 μM) (Figure 3). All of the described results here indicate that the strength of stabilizing poly(dA)·2poly(dT) increases in the following order: neomycin < **1** < **3** < **4** < **2**. Interestingly, the strength of stabilizing poly(dA)·2poly(dT) by intercalators **5**, **6**, **7**, and **8** at 4 μM showed the same order exhibited by intercalator−neomycin conjugates (Tables 1 and 2 of the Supporting Information), suggesting that the increasing surface area of the intercalator moiety is clearly an important factor in recognition of the DNA triplex.

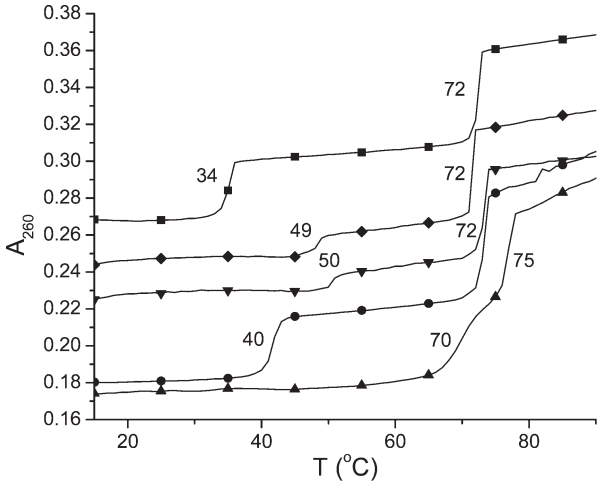

FIGURE 3: Representative UV melting profiles of poly(dA)·2poly(dT) at 260 nm in the absence (■) and presence of neomycin [4 μM (◆)], neomycin and **7** [4 μM each (▼)], **7** [4 μM (●)], and **3** [4 μM (▲)]. Experimental conditions: sodium cacodylate buffer (10 mM, pH 6.8), KCl (150 mM), and EDTA (0.5 mM). [DNA] = 15 μM per base triplet. The *y*-axis has been artificially offset to differentiate the melting curves.

Competition Dialysis of Intercalator−Neomycin Conjugates with Different Structures of Nucleic Acids. Competition dialysis is a quick and convenient method developed by Chaires (*47*, *54*) for simultaneously determining the binding preference of ligands for different structures of nucleic acids. The nucleic acid solutions (75 μM per monomeric unit of each polymer) in mini-dialysis units are allowed to equilibrate against a large excess of the desired ligand (1 μM). After the bound ligand had dissociated from nucleic acids via use of a surfactant (SDS), the concentration of the ligand was measured spectroscopically. The amount of detected ligand in each nucleic acid solution corresponds to its binding affinity for this nucleic acid. Our previous competition dialysis study revealed that **2** binds preferentially to DNA or RNA triple-helical structures while having minimum binding to the corresponding single-stranded and duplex nucleic acids. In this study, competition dialysis experiments with **1**, **3**, and **4** as well as their corresponding intercalators (**5**, **7**, and **8**) against 20 different types of nucleic acids, including G-quadruplex and triplex, were conducted.

The concentration of the ligand in each individual nucleic acid solution is determined via subtraction of the ligand concentration in the calf thymus DNA solution, a typical B-form nucleic acid structure (Figure 4). Calf thymus DNA is chosen because according to the UV denaturation studies, these intercalator−neomycin conjugates have minimal binding affinity for it. Our results show that in general, compounds **1**, **3**, and **4** do not bind to single-stranded nucleic acids. Just like **2**, all three intercalator−neomycin conjugates tested here bind preferentially to poly(dA)·2poly(dT) while having little binding affinity for poly(dA)·poly(dT). This observation unambiguously supports our previous conclusions that intercalator−neomycin conjugates favor triple-helical DNA structures. Compounds **1** and **4** bind to

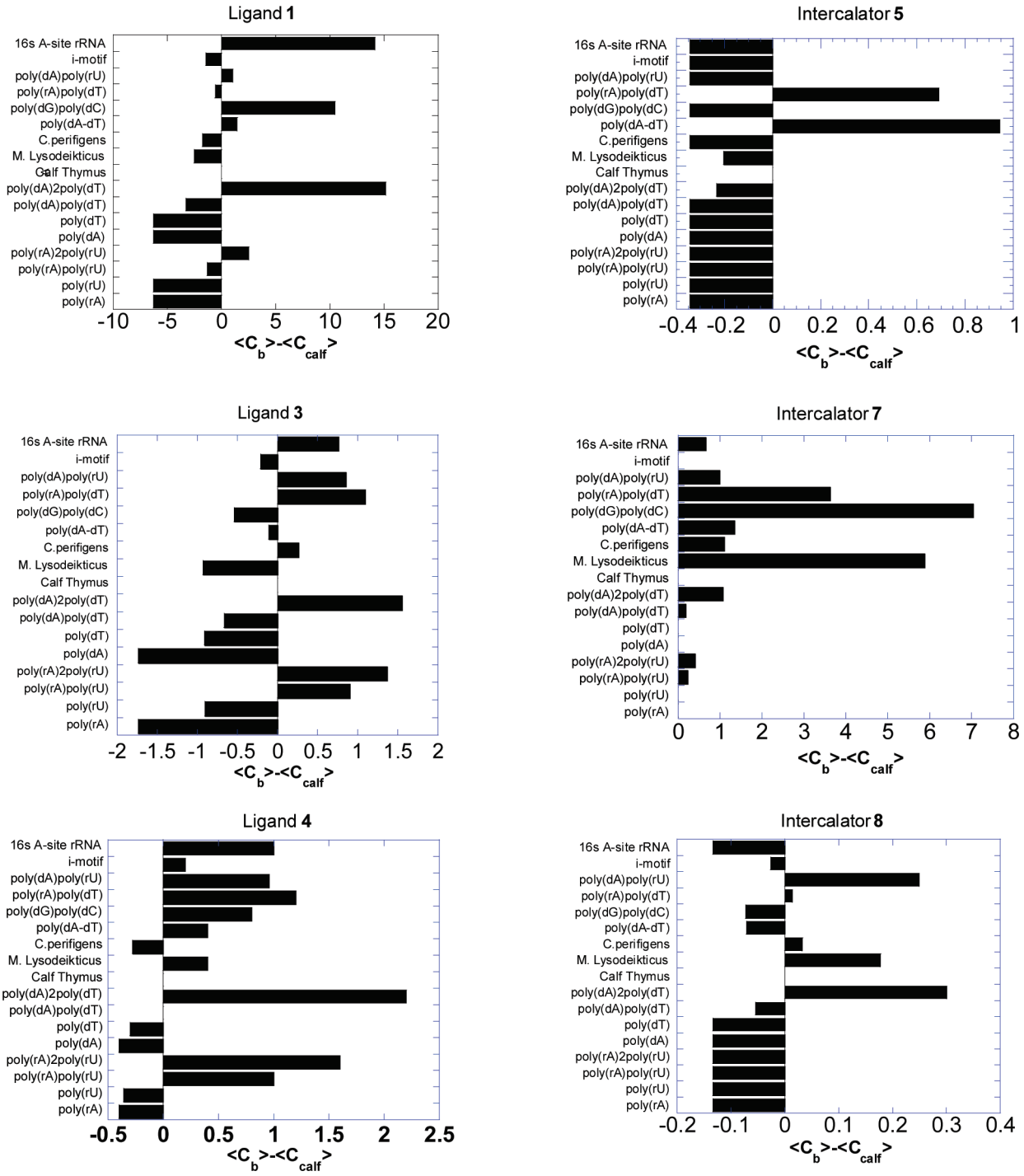

FIGURE 4: Competition dialysis results of **1**, **3**, and **4** as well as their corresponding intercalators **5**, **7**, and **8** (1 μM) with various types of nucleic acids (75 μM). Buffer: Na_2HPO_4 (6 mM), NaH_2PO_4 (2 mM), Na_2EDTA (1 mM), NaCl (185 mM), and pH 7.0.

poly(dG)·poly(dC), while **3** does not bind to it at all. All three intercalator−neomycin conjugates to some extent have binding affinity for DNA−RNA hybrid sequences, such as poly(dA)·poly(rU), which are know to be A-form nucleic acid structures (*49*).The competition dialysis results for the intercalators (**5**, **7**, and **8**) show patterns different from those of **1**, **3**, and **4**, suggesting that the selectivity in binding of **1**, **3**, and **4** to different nucleic acids results from the combination of groove binding and stacking interactions, not simply from the base stacking interactions of the intercalator.

Determining the Binding Site Size of Intercalator−Neomycin Conjugates with Poly(dA)·2Poly(dT) Using UV Thermal Denaturation, CD, and Fluorescence Spectroscopy. To understand the binding of our intercalator−neomycin conjugates with poly(dA)·2poly(dT), we sought to investigate the binding site sizes of **1**−**4** with poly(dA)·2poly(dT) using UV thermal denaturation and circular dichroism (CD) spectroscopy. Binding of the intercalator−neomycin conjugates (**1**−**4**) with poly(dA)·2poly(dT) slightly altered the conformation of the DNA triplex secondary structure, which was consequently detected by circular dichroism spectroscopy. A much larger change in T_m was observed using thermal denaturation studies (Table 2). T_m changes varied linearly with an increase in concentration of the intercalator−neomycin conjugates, and a

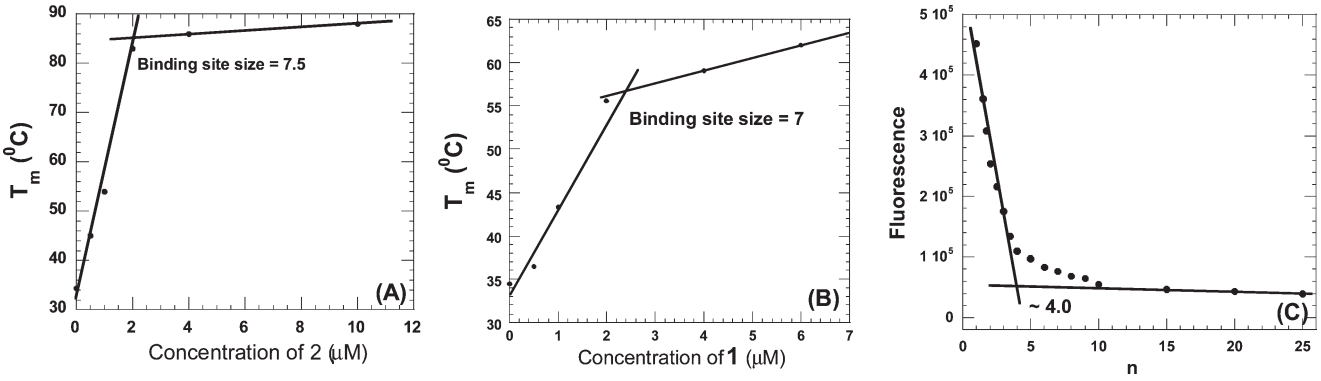

FIGURE 5: (A and B) Representative plots for the determination of binding site sizes of intercalator−neomycin conjugates with poly(dA)·2poly(dT) as determined by UV thermal denaturation. (C) Plot for the determination of the binding site of poly(dA)·2poly(dT) and naphthalene diimide. The graph shows the change in fluorescence of naphthalene diimide when it is titrated with poly(dA)·2poly(dT). Naphthalene diimide was excited at 356 nm, and the emission scans were recorded from 370 to 500 nm: 15 μM poly(dA)·poly(dT)/base triplet, 0.5−15 μM naphthalene diimide, 10 °C. *n* is the number of base triplets per drug. Buffer conditions: sodium cacodylate (10 mM), EDTA (0.5 mM), KCl (150 mM), and pH 5.5.

plot of T_m versus ligand concentration was made to determine the binding site size. A transition point resulting from the slope change was clearly observed in all of the plots, when the primary available sites in poly(dA)·2poly(dT) were saturated by the intercalator−neomycin conjugate. Our results suggest that the binding site sizes of **1**−**4** with poly(dA)·2poly(dT) are 7, 7.5, 7.5, and 7.5, respectively (Figure 5). The values of binding site size described here are reasonable compared to that of neomycin and conjugates (~6−6.5) reported previously using CD spectroscopy (*27*, *44*, *45*). The observed similarity in binding site sizes implies a similarity in the binding modes of compounds **1**−**4** with poly(dA)·2poly(dT).

Extrapolating Thermodynamic Parameters from the Interactions between Intercalator−Neomycin Conjugates and Poly(dA)·2Poly(dT). Our ultimate understanding of interactions between intercalator−neomycin conjugates and poly(dA)·2poly(dT) is achieved by acquiring a complete set of thermodynamic parameters. A method for extrapolating thermodynamic parameters from experimental data was developed and optimized by McGhee and others (*46*, *55*); they used the following equation.

$$\frac{1}{T_{m0}} - \frac{1}{T_m} = \frac{R}{n(\Delta H_{HS})} \ln(1 + K_{T_m} L)$$

where T_{m0} is the melting temperature representing the dissociation of the DNA triplex into the duplex in the absence of ligand, T_m is the melting temperature representing the dissociation of the DNA triplex into the duplex in the presence of an intercalator−neomycin conjugate, R is the gas constant, ΔH_{HS} is the enthalpy change corresponding to the dissociation of the DNA triplex into the duplex in the absence of ligand, L is the free ligand concentration at T_m which is estimated to be one-half of the total drug concentration, and n is the binding site size. The melting temperatures were determined using UV spectroscopy as described above. The enthalpy change (ΔH_{HS}) was measured using differential scanning calorimetry (DSC), in which the heat produced from the dissociation of the DNA triplex was plotted as a function of temperature (20−90 °C). The binding site size was obtained from UV thermal denaturation and CD titration experiments as described above. After this equation had been solved, the association constant at T_m (K_{T_m}) in the presence of the intercalator−neomycin conjugate at a desired concentration was obtained. The more meaningful and useful association constants (K_T) at different temperatures for analysis of interactions between the intercalator−neomycin conjugate and poly(dA)·2poly(dT) were further derived from the following integrated van't Hoff equation using the calculated K_{T_m} values.

$$K_T = \frac{K_{T_m}}{e^{-\Delta H_T/R(1/T_m - 1/T)} e^{\Delta C_p T(1/T_m - 1/T)} \left(\frac{T_m}{T}\right)^{\Delta C_p/R}}$$

where ΔH_T is the observed enthalpy change associated with the binding of an intercalator−neomycin conjugate to poly(dA)·2poly(dT) and ΔC_p is the heat capacity change for binding. ΔH_T was determined using isothermal titration calorimetry (ITC), in which small aliquots of a buffered intercalator−neomycin conjugate were injected into a solution containing a large excess of poly(dA)·2poly(dT) in terms of possible numbers of binding sites. ΔC_p was derived from the slope of the linear relationship in which the binding enthalpy (ΔH_T) was plotted as a function of temperature (T).

All of the experiments used for calculations of thermodynamic parameters were conducted at two different pH values (6.8 and 5.5). The ΔH_{HS} values measured by DSC for the dissociation of poly(dA)·2poly(dT) into poly(dA)·poly(dT) and poly(dT) at pH 5.5 and 6.8 were 1.67 and 1.59 kcal/mol, respectively (Figure 6), suggesting that poly(dA)·2poly(dT) was more stable at a lower pH. This observation is consistent with the common belief that the stability of the DNA triplex increases with a decrease in pH because of suppression of the electrostatic repulsions between DNA backbones under lower-pH conditions. A similar trend was observed for the dissociation of poly(dA)·poly(dT) into poly(dA) and poly(dT), in which the ΔH_{HS} value at pH 5.5 (5.00 kcal/mol) was 150 cal/mol higher than that at pH 6.8 (4.87 cal/mol).

Figure 7a shows the CD spectra of the preformed poly(dA)·poly(dT) duplex and poly(dA)·2poly(dT) triplex in the absence (scans a and c) and presence of the tightest binding ligand **2**, BQQ−neomycin (scans b and d). The duplex and triplex DNA have signature CD spectra which have been preserved upon addition of the conjugate, suggesting that little conformational change takes place when drug is added. Figure 7a shows that when ligand **2** (BQQ−neomycin) binds to the duplex or triplex, no red or blue shift is observed in the CD spectrum of the preformed duplex or triplex. Figure 7b shows the continuous variation experiments with poly(dA) and poly(dT) in the absence

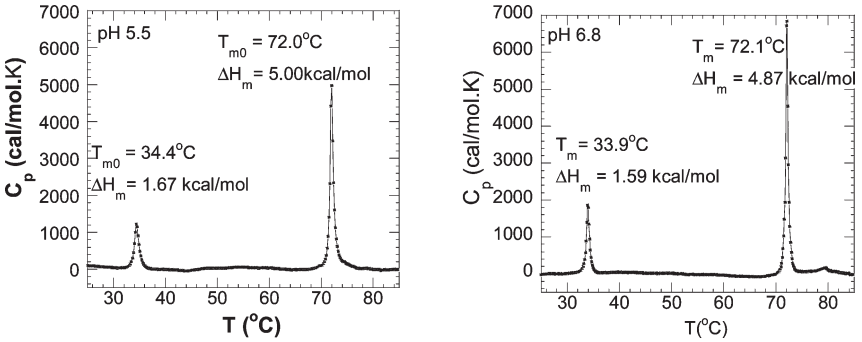

FIGURE 6: DSC melting profile of poly(dA)·2poly(dT) in the absence of binding ligand at pH 5.5 (left) and pH 6.8 (right). Experimental conditions: sodium cacodylate (10 mM), EDTA (0.5 mM), and KCl (150 mM).

and presence of drug **3**. All intercalators and conjugates exhibit similar minima at 66% dT, suggesting that the three-strand DNA triplex is present in solution in the absence and presence of the drugs.

ITC experiments were conducted to determine the enthalpy changes in the binding of intercalator−neomycin conjugates to poly(dA)·2poly(dT) at pH 5.5 and 6.8 (Figures 13−20 of the Supporting Information). The preformed DNA triplex solution was incubated in a sample cell at the temperatures which were lower than 20 °C to ensure the presence of DNA triplex (T_m = 34 °C). The enthalpy changes (ΔH_T) were recorded as a heat burst curve when small portions of the buffered intercalator−neomycin conjugate were injected into the DNA solution. The area under each heat burst curve was integrated and recorded as the ΔH_T values. For instance, when the pH of the solution was 5.5, the ΔH_T values at 10 °C for neomycin, **1**, **2**, **3**, and **4** were -6.4 ± 0.1, -3.2 ± 0.1, -6.8 ± 0.1, -10.9 ± 0.2, and -15.9 ± 0.4 kcal/mol, respectively (Table 3). Under this condition, the ΔH_T values increased in the following order: **1** < **3** < **4** < **2** (which is consistent with the order of DNA triplex stabilization derived from UV denaturation experiments). A similar trend was also observed when intercalator−neomycin conjugates were injected into the poly(dA)·2poly(dT) solution at different temperatures and pH values (Table 3). The enthalpy change in the binding of neomycin to poly(dA)·2poly(dT) at pH 6.8 was somewhat different from the trend observed in the UV denaturation experiments. Our UV melting studies suggest that **1** has a stronger stabilization effect on poly(dA)·2poly(dT) than neomycin at pH 6.8. For instance, the melting temperature of poly(dA)·2poly(dT) in the presence of **1** (4 μM) was 24 °C higher than that in the presence of neomycin. However, at pH 6.8, the enthalpy change for the binding of **1** to poly(dA)·2poly(dT) was 3.2 kcal/mol lower than that for the binding of neomycin to poly(dA)·2poly(dT) even though **1** has greater DNA triplex stabilization than neomycin. In contrast, at pH 5.5, the enthalpy change for the binding of **1** to poly(dA)·2poly(dT) was 0.9 kcal/mol greater than that for the binding of neomycin to poly(dA)·2poly(dT), which was consistent with the order in which **1** stabilizes triplex more. In addition, the enthalpy changes for the binding of the intercalator−neomycin conjugate with poly(dA)·2poly(dT) at pH 6.8 were much greater than that for the corresponding binding at pH 5.5. This observation is attributed to the binding-linked neomycin protonation heat. The amino groups of neomycin, according to their pK_a values, are not completely protonated at pH 6.8. The heat produced from such amine protonation at pH 6.8 results in an overestimation of enthalpy changes (*56*). The enthalpy change measured at pH 5.5 reflects more of an intrinsic interaction between the intercalator−neomycin conjugate and poly(dA)·2poly(dT) because neomycin is substantially protonated at this pH value and thus the protonation heat is minimized. However, studying such a binding event at pH 5.5 can lead to some practical problems. The interactions between these conjugates and poly(dA)·2poly(dT) intend to become more entropy-driven at low pH; therefore, the intensity of ITC signals decreases dramatically, necessitating the use of higher concentrations of samples.

To calculate the ΔC_p values, the enthalpy changes (ΔH_T) were plotted versus temperature and fitted via linear regression analysis. The slope of linear fitting represents the ΔC_p in the binding of intercalator−neomycin conjugates to poly(dA)·2poly(dT) under this experimental condition. In all cases, negative ΔC_p values were observed at pH 6.8 and 5.5 and the ΔC_p values are in general more negative at pH 6.8 than at pH 5.5 (Tables 3 and 4). Protonation heats at pH 6.8 yield a much higher ΔC_p value. In contrast, the relatively low ΔC_p values at pH 5.5 indicate a more intrinsic drug−triplex interaction. Additionally, the enthalpy changes in the binding of **3** and **4** with triplex poly(dA)·2poly(dT) were −3.7 and −7.8 kcal/mol greater, respectively, than those with the duplex poly(dA)·poly(dT), suggesting that interactions between the intercalator−neomycin conjugate and the DNA triplex are more enthalpy-driven than those with the DNA duplex.

The binding constant of the intercalator−neomycin conjugate with poly(dA)·2poly(dT) was then derived using all the parameters described above. At pH 5.5, all intercalator−neomycin conjugates seemed to bind poly(dA)·2poly(dT) more tightly than neomycin. The calculated binding constants increased in the order neomycin < **1** < **3** < **4** < **2**, with values of $(2.7 \pm 0.3) \times 10^8$ M^{-1} for **2**, $(3.7 \pm 0.1) \times 10^7$ M^{-1} for **3**, $(5.5 \pm 0.3) \times 10^6$ M^{-1} for **4**, $(1.9 \pm 0.1) \times 10^6$ M^{-1} for **1**, and $(2.4 \pm 0.1) \times 10^5$ M^{-1} for neomycin (Table 3). The binding constant of **2** with poly(dA)·2poly(dT) is $(2.7 \pm 0.3) \times 10^8$ M^{-1}, which is ~1000-fold higher than that of neomycin. This observed high binding constant of **2** is consistent with our previously published result which showed that **2** is a very potent DNA triplex binding ligand. The rationally designed triplex-specific binding ligand, BQQ in **2**, may play an important role in promoting significant DNA triplex binding. The binding constant of **2** with poly(dA)·2poly(dT) is ~7.3-, ~49-, and ~142-fold higher than those of **4**, **3**, and **1**, respectively. These data, in addition to our FID AC_{50} values, allow us to quantitate the relative strength of binding of the intercalators to poly(dA)·2poly(dT). The larger the surface area of the intercalator, the higher the DNA triplex binding affinity of its neomycin conjugate. Pyrene itself does not stabilize DNA

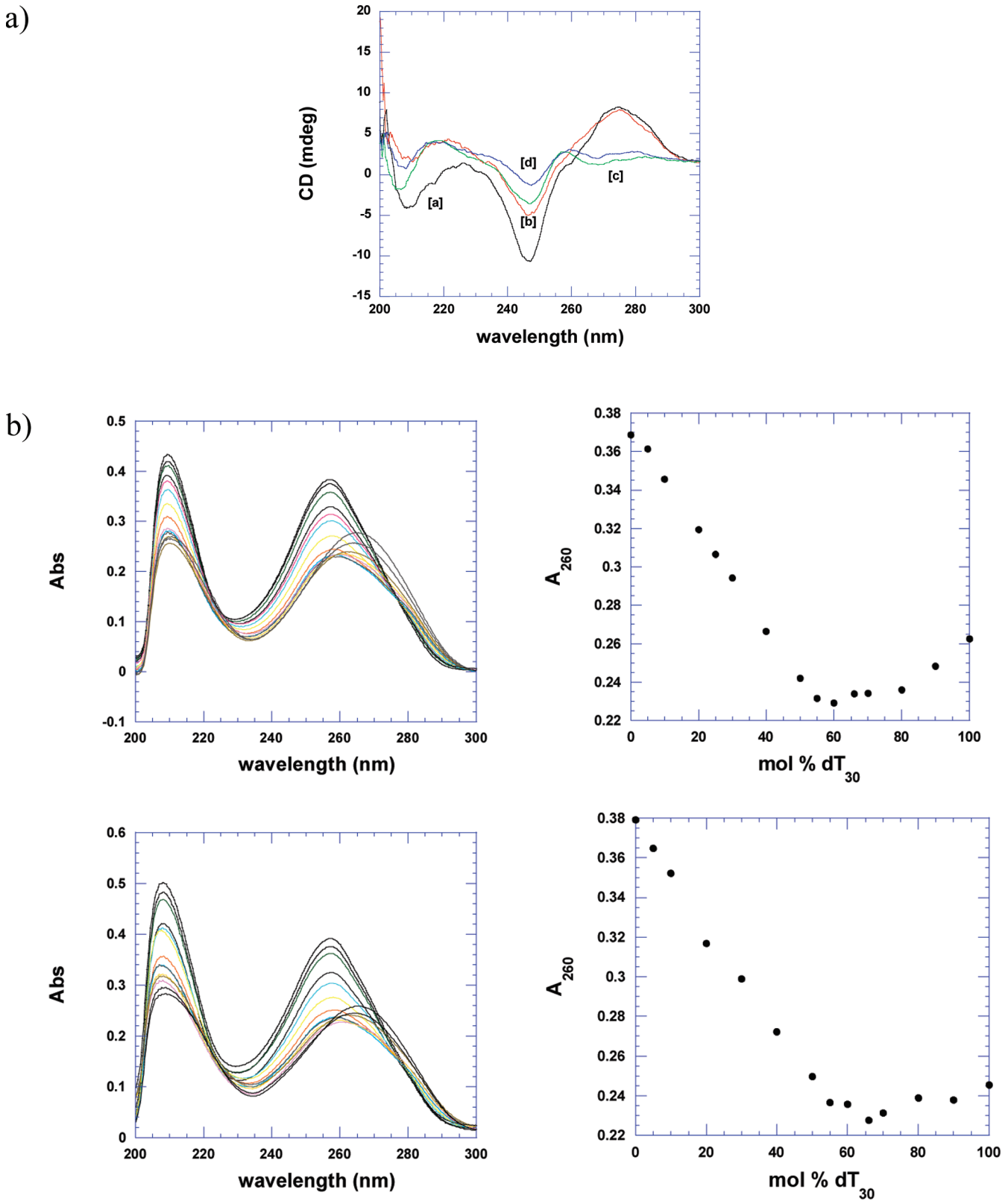

FIGURE 7: CD scans for the poly(dA)·poly(dT) duplex and the poly(dA)·2poly(dT) triplex in the absence and presence of **2** (BQQ−neomycin). (a) Poly(dA)·2poly(dT) triplex (no ligand) [a], poly(dA)·2poly(dT) triplex (0.13 equiv of **2**) [b], poly(dA)·poly(dT) duplex (no ligand) [c], and poly(dA)·poly(dT) duplex (0.13 equiv of **2**) [d]. Experimental conditions: sodium cacodylate (10 mM), EDTA (0.5 mM), KCl (150 mM), 10 °C, and pH 5.5. (b) Continuous variation scans (left) and A_{260} plot (right) of dA_{30} (1 μM/base) and dT_{30} (1 μM/base) in the absence of drug (top) and presence of napthalenediimide−neomycin conjugate **3** (r_{bd} = 7) (bottom). Experimental conditions: sodium cacodylate (10 mM), EDTA (0.5 mM), KCl (150 mM), 15 °C, and pH 5.5.

triplexes; therefore, its conjugate **1** has the weakest triplex binding ability among the four. The slight discrepancy between FID results and calorimetric data, when comparing the affinities, can be attributed to the differences in the nature and sensitivities of the measurements, given that the affinities are quite comparable. The FID assay, which indirectly measures the ligand affinities,

Table 3: Thermodynamic Profiles of Intercalator−Neomycin Conjugates (**1**−**4**) and Intercalator **7** with Poly(dA)·2Poly(dT) at pH 5.5[a]

ligand	[KCl] (mM)	ΔH_{wc} (kcal/mol)	T_{m0} (°C)	T_m (°C)	n	$\Delta H_{(10\ °C)}$ (kcal/mol)	$\Delta H_{(15\ °C)}$ (kcal/mol)	$\Delta H_{(20\ °C)}$ (kcal/mol)	ΔC_p (cal mol^{-1} K^{-1})	$K_{T(20\ °C)}$ (M^{-1})
neomycin	140	1.70	31.4	34.4	6.8	−0.6 ± 0.1 (12 °C)	−	−1.31 ± 0.02	−87 ± 4	(2.4 ± 0.1) × 10^5
1	150	1.67	33.8	49.5	7	−1.5 ± 0.1	−	−1.64 ± 0.02	−10 ± 3	(1.9 ± 0.1) × 10^6
3	150	1.67	33.8	55.4	7.5	−2.4 ± 0.1	−2.6 ± 0.1	−2.8 ± 0.1	−40 ± 20	(5.5 ± 0.3) × 10^6
4	150	1.67	33.8	64.0	7.5	−5.4 ± 0.2	−6.1 ± 0.2	−6.4 ± 0.1	−110 ± 15	(3.7 ± 0.1) × 10^7
2	150	1.67	33.8	68.8	7.5	−7.5 ± 0.4	−8.5 ± 0.4	−9.7 ± 0.2	−220 ± 20	(2.7 ± 0.3) × 10^8
7	150	1.67	31.0	37.2	4	−1.4 ± 0.1[b]	−0.38 ± 0.07	−0.81 ± 0.01	−131	1.89 × 10^5

[a]Experimental condition: sodium cacodylate (10 mM), EDTA (0.5 mM), and KCl (150 mM). [b]Calculated at 23 °C.

Table 4: Thermodynamic Profiles of Intercalator−Neomycin Conjugates (**1**−**4**) with Poly(dA)·2Poly(dT) at pH 6.8[a]

ligand	[KCl] (mM)	ΔH_{wc} (kcal/mol)	T_{m0} (°C)	T_m (°C)	n	$\Delta H_{(10\ °C)}$ (kcal/mol)	$\Delta H_{(20\ °C)}$ (kcal/mol)	$\Delta H_{(5\ °C)}$ (kcal/mol)	ΔC_p (cal mol^{-1} K^{-1})	$K_{T(20\ °C)}$ (M^{-1})
neomycin	150	1.59	34.4	49.5	6.5	−6.4 ± 0.1	−7.5 ± 0.2	−8.2 ± 0.04	−116 ± 4	−
1	150	1.59	34.4	58.0	7	−3.2 ± 0.1	−3.7 ± 0.1	−	−45 ± 1	−
3	150	1.59	34.4	65.0	7.5	−6.8 ± 0.1	−7.8 ± 0.1	−8.3 ± 0.8	−104 ± 10	−
4	150	1.59	34.4	68.0	7.5	−10.9 ± 0.2	−12.7 ± 0.2	−14.5 ± 0.1	−231 ± 6	−
2	150	1.59	34.4	85.0	7.5	−15.9 ± 0.4	−19.3 ± 0.4	−21.1 ± 0.4	−346 ± 13	−

[a]Experimental condition: sodium cacodylate (10 mM), EDTA (0.5 mM), and KCl (150 mM).

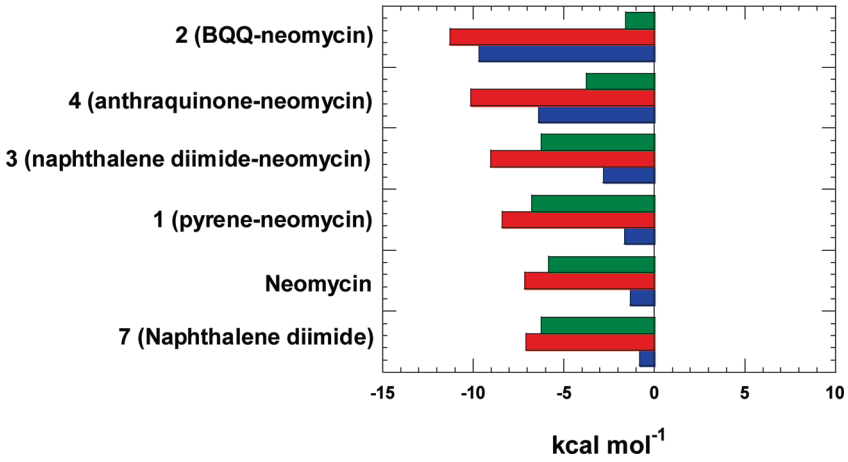

FIGURE 8: Thermodynamics of binding interactions of ligands with the poly(dA)·2poly(dT) triplex at pH 5.5. Red bars represent ΔG, blue bars ΔH, and green bars $T\Delta S$. Experimental conditions: sodium cacodylate (10 mM), EDTA (0.5 mM), and KCl (150 mM).

shows a 2−4-fold higher affinity for **1** over **3**, whereas data from Table 3 show the opposite trend, with **3** showing a 2-fold higher affinity. Additionally, the FID measurements were performed at pH 6.8, whereas the affinities listed in Table 3 are reported at pH 5.5. When the FID experiments were repeated at pH 5.5, similar trends were observed, with **3** (AC_{50} = 408 ± 70 nM) showing a higher AC_{50} than **1** (AC_{50} = 240 ± 20 nM). The UV thermal denaturation temperatures at both pH 6.8 and 5.5 (Tables 2 and 3) clearly show a much larger change in $T_{m3\rightarrow2}$ for **3** over **1** (70 °C vs 50 °C at pH 6.8 and 55.9 °C vs 49 °C at pH 5.5), suggesting that **3** stabilizes the DNA triplex better than **1** at the two pH values.

Figure 8 shows the distribution of thermodynamic properties of ligand−triplex interactions as bar graphs. The free energy for each of the ligand has been calculated from the binding constant by using the Gibbs free energy equation. Free energy change (red bars), enthalpy change (blue bars), and entropic contributions (green bars) help summarize the contribution of the individual ligands as well as the conjugates. Three different classes of ligands are represented in the figure with respect to binding mode. Neomycin is a major groove binder; naphthalene diimide is a well-known intercalator, and neomycin conjugates bind through the dual recognition mode (major groove and intercalation). The plot in Figure 8 is a good starting point for understanding the contribution of thermodynamic properties during the drug−DNA binding interactions. It is clear from the figure that binding of neomycin (groove binder) as well as naphthalene diimide (intercalator) is largely driven by enthalpy contributions. As we go from **1** (pyrene−neomycin) to **2** (BQQ−neomycin), an increase in intercalator surface area leads to an increase in the enthalpy of interaction, which clearly leads to a more negative free energy of binding. However, as seen from the free energies of interaction of neomycin, **7**, and **3**, the free energy $\Delta G_{\mathbf{3}-triplex}$ is not a sum of free energies $\Delta G_{neomycin-triplex}$ and $\Delta G_{\mathbf{7}-triplex}$, leading to a $\Delta G_{coupling}$ of ∼5 kcal/mol. While $\Delta H_{\mathbf{3}-triplex}$ increases substantially, the corresponding increase in $\Delta S_{\mathbf{3}-triplex}$ is not observed, suggesting that the conjugate pays an entropic cost of covalently bridging neomycin with the intercalator with the given linker length. As we proceed to the higher-affinity conjugates **2** and **4**, the entropic contribution to $\Delta G_{complexation}$ decreases substantially. The thermodynamics of interaction of ligands **5**, **6**, and **8** with the

triplex could not be performed because of the poor solubility of these compounds in aqueous solution. Further studies with different linker lengths will be beneficial in maximizing the free energies of interaction of the dual binding modes and are currently being explored in our laboratories.

CONCLUSIONS

Decades of work in the recognition of DNA triplexes have led to the design of intercalators that preferentially bind to DNA triplexes, while minimizing the binding to the DNA duplex. Addition of a groove binding DNA triplex selective ligand such as neomycin has allowed us to achieve DNA triplex affinities that would be difficult to attain with a univalent binding mode without sacrificing selectivity. Our results here provide a measure of quantification of triplex binding when the ligand surface area is increased in the following order: pyrene < naphthalene diimide anthraquinone < BQQ. It is not a surprise that **2** is the most potent DNA triplex stabilizing agent among all the intercalator−neomycin conjugates in our study because the BQQ moiety (**6**) is known as a rationally designed DNA triplex-specific binding ligand. All of the other intercalators (pyrene, naphthalene diimide, and anthraquinone) bind to the DNA duplex as well as the DNA triplex to some extent. The conjugates containing the intercalator and neomycin enhance the binding affinity of the DNA triplex via a possible cooperative binding mode. Such a "dual binding mode" may be useful in guiding the design of novel DNA triplex binding ligands (and perhaps other nucleic acids). The thermodynamic data also raise the possibility of tuning the DNA triplex binding strength of neomycin conjugates by simply swamping the intercalator moiety. A large data bank of DNA intercalators has already been established; therefore, preparation of such conjugates for screening the nucleic acid binding ligands is practical. Inspection of the ligand−triplex interaction thermodynamics shows a clear additive effect of enthalpies of interaction, and future studies with linker length optimization can lead to even higher-affinity ligands.

SUPPORTING INFORMATION AVAILABLE

NMR spectra of **3** and **4**, spectra for ITC experiments of compounds **1**−**4** titrating into a large excess of poly(dA)·2poly(dT) at pH 5.5 and 6.8, and ΔC_p plots. This material is available free of charge via the Internet at http://pubs.acs.org.

REFERENCES

1. Felsenfeld, G., Davies, D., and Rich, A. (1957) Formation of a Three Stranded Polynucleotide Molecule. *J. Am. Chem. Soc. 79*, 2023–2024.
2. Radhakrishnan, I., and Patel, D. J. (1994) Solution Structure of a Pyrimidine·Purine·Pyrimidine DNA Triplex Containing T·AT, C^+·GC and G·TA Triples. *Structure 2*, 17–32.
3. Praseuth, D., Guieysse, A. L., and Helene, C. (1999) Triple Helix Formation and the Antigene Strategy for Sequence-Specific Control of Gene Expression. *Biochim. Biophys. Acta 1489*, 181–206.
4. Beal, P. A., and Dervan, P. B. (1991) Second Structural Motif for Recognition of DNA by Oligonucleotide-Directed Triple-Helix Formation. *Science 251*, 1360–1363.
5. Chen, F. M. (1991) Intramolecular Triplex Formation of the Purine·Purine·Pyrimidine Type. *Biochemistry 30*, 4472–4479.
6. Radhakrishnan, I., and Patel, D. J. (1993) Solution Structure of a Purine·Purine·Pyrimidine DNA Triplex Containing G·GC and T·AT Triplexes. *Structure 1*, 135–152.
7. Michel, D., Chatelain, G., Herault, Y., and Brun, G. (1992) The Long Repetitive Polypurine Polypyrimidine Sequence $(Ttccc)_{48}$ Forms DNA Triplex with Pu-Pu-Py Base Triplets In Vivo. *Nucleic Acids Res. 20*, 439–443.
8. Agazie, Y. M., Lee, J. S., and Burkholder, G. D. (1994) Characterization of a New Monoclonal Antibody to Triplex DNA and Immunofluorescent Staining of Mammalian Chromosomes. *J. Biol. Chem. 269*, 7019–7023.
9. Kopel, V., Pozner, A., Baran, N., and Manor, H. (1996) Unwinding of the Third Strand of a DNA Triple Helix, a Novel Activity of the SV40 Large T-Antigen Helicase. *Nucleic Acids Res. 24*, 330–335.
10. Spitzner, J. R., Chung, I. K., and Muller, M. T. (1995) Determination of 5′ and 3′ DNA Triplex Interference Boundaries Reveals the Core DNA Binding Sequence for Topoisomerase II. *J. Biol. Chem. 270*, 5932–5943.
11. Cooney, M., Czernuszewicz, G., Postel, E. H., Flint, S. J., and Hogan, M. E. (1988) Site-Specific Oligonucleotide Binding Represses Transcription of the Human c-Myc Gene in Vitro. *Science 241*, 456–459.
12. Postel, E. H., Flint, S. J., Kessler, D. J., and Hogan, M. E. (1991) Evidence that a Triplex-Forming Oligodeoxyribonucleotide Binds to the c-Myc Promoter in HeLa Cells, Thereby Reducing c-Myc mRNA Levels. *Proc. Natl. Acad. Sci. U.S.A. 88*, 8227–8231.
13. Grigoriev, M., Praseuth, D., Guieysse, A. L., Robin, P., Thuong, N. T., Helene, C., and Harel-Bellan, A. (1993) Inhibition of Gene Expression by Triple Helix-Directed DNA Cross-Linking at Specific Sites. *Proc. Natl. Acad. Sci. U.S.A. 90*, 3501–3505.
14. Grigoriev, M., Praseuth, D., Robin, P., Hemar, A., Saison-Behmoaras, T., Dautry-Varsat, A., Thuong, N. T., Helene, C., and Harel-Bellan, A. (1992) A Triple Helix-Forming Oligonucleotide-Intercalator Conjugate Acts as a Transcriptional Repressor Via Inhibition of NF κB Binding to Interleukin-2 Receptor a-Regulatory Sequence. *J. Biol. Chem. 267*, 3389–3395.
15. Murray, J. A. H. (1992) Antisense RNA and DNA, Wiley-Liss, New York.
16. Aviño, A., Grimau, M. G., Frieden, M., and Eritja, R. (2004) Synthesis and Triple-Helix-Stabilization Properties of Branched Oligonucleotides Carrying 8-Aminoadenine Moieties. *Helv. Chim. Acta 87*, 303–316.
17. Sollogoub, M., Dominguez, B., Brown, T., and Fox, K. R. (2000) Synthesis of a Novel Bis-Amino-Modified Thymidine Monomer for use in DNA Triplex Stabilisation. *Chem. Commun. 23*, 2315–2316.
18. Kawai, K., Saito, I., and Sugiyama, H. (1998) Stabilization of Hoogsteen Base Pairing by Introduction of NH2 Group at the C8 Position of Adenine. *Tetrahedron Lett. 39*, 5221–5224.
19. Gianolio, D. A., Segismundo, J. M., and McLaughlin, L. W. (2000) Tethered Naphthalene Diimide-Based Intercalators for DNA Triplex Stabilization. *Nucleic Acids Res. 28*, 2128–2134.
20. Sun, J., Carestier, T., and Hélène, C. (1996) Oligonucleotide Directed Triple Helix Formation. *Curr. Opin. Struct. Biol. 6*, 327–333.
21. Baudoin, O., Marchand, C., Teulade-Fichou, M.-P., Vigneron, J.-P., Sun, J.-S., Garestier, T., Helene, C., and Lehn, J.-M. (1998) Stabilization of DNA Triple Helices by Crescent-Shaped Dibenzophenanthrolines. *Chem.—Eur. J. 4*, 1504–1508.
22. Robles, J., and McLaughlin, L. W. (1997) DNA Triplex Stabilization using a Tethered Minor Groove Binding Hoechst 33258 Analogue. *J. Am. Chem. Soc. 119*, 6014–6021.
23. Scaria, P. V., and Shafer, R. H. (1991) Binding of Ethidium Bromide to a DNA Triple Helix. *J. Biol. Chem. 266*, 5417–5423.
24. Pilch, D. S., Martin, M. T., Nguyen, C. H., Sun, J. S., Bisagni, E., Garestier, T., and Helene, C. (1993) Self-Association and DNA-Binding Properties of Two Triple Helix-Specific Ligands: Comparison of a Benzo[e]Pyridoindole and a Benzo[g]Pyridoindole. *J. Am. Chem. Soc. 115*, 9942–9951.
25. Escude, C., Nguyen, C. H., Mergny, J.-L., Sun, J.-S., Bisagni, E., Garestier, T., and Helene, C. (1995) Selective Stabilization of DNA Triple Helices by Benzopyridoindole Derivatives. *J. Am. Chem. Soc. 117*, 10212–10219.
26. Arya, D. P., Jr., Coffee, R. L., Jr., Willis, B., and Abramovitch, A. I. (2001) Aminoglycoside-Nucleic Acid Interactions: Remarkable Stabilization of DNA and RNA Triple Helices by Neomycin. *J. Am. Chem. Soc. 123*, 5385–5395.
27. Arya, D. P., Micovic, L., Charles, I., Jr., Coffee, R. L., Jr., Willis, B., and Xue, L. (2003) Neomycin Binding to Watson-Hoogsteen (W-H) DNA Triplex Groove: A Model. *J. Am. Chem. Soc. 125*, 3733–3744.
28. Willis, B., and Arya, D. P. (2009) Triple Recognition of B-DNA. *Bioorg. Med. Chem. Lett. 19*, 4974–4979.
29. Willis, B., and Arya, D. P. (2006) Major Groove Recognition of DNA by Carbohydrates. *Curr. Org. Chem. 10*, 663–673.
30. Willis, B., and Arya, D. P. (2006) An Expanding View of Aminoglycoside-Nucleic Acid Recognition. *Adv. Carbohydr. Chem. Biochem. 60*, 251–302.

31. Arya, D. P., and Willis, B. (2003) Reaching into the Major Groove of B-DNA: Synthesis and Nucleic Acid Binding of a Neomycin-Hoechst 33258 Conjugate. *J. Am. Chem. Soc. 125*, 12398–12399.
32. Shaw, N. N., and Arya, D. P. (2008) Recognition of the Unique Structure of DNA:RNA Hybrids. *Biochimie 90*, 1026–1039.
33. Shaw, N. N., Xi, H., and Arya, D. P. (2008) Molecular Recognition of a DNA:RNA Hybrid: Sub-Nanomolar Binding by a Neomycin-Methidium Conjugate. *Bioorg. Med. Chem. Lett. 18*, 4142–4145.
34. Arya, D. P. (2005) Aminoglycoside-Nucleic Acid Interactions: The Case for Neomycin. *Top. Curr. Chem. 253*, 149–178.
35. Arya, D. P., Coffee, R. L., Jr., and Charles, I. (2001) Neomycin-Induced Hybrid Triplex Formation. *J. Am. Chem. Soc. 123*, 11093–11094.
36. Charles, I., Xi, H., and Arya, D. P. (2007) Sequence-Specific Targeting of RNA with an Oligonucleotide-Neomycin Conjugate. *Bioconjugate Chem. 18*, 160–169.
37. Charles, I., Xue, L., and Arya, D. P. (2002) Synthesis of Aminoglycoside-DNA Conjugates. *Bioorg. Med. Chem. Lett. 12*, 1259–1262.
38. Xi, H., Gray, D., Kumar, S., and Arya, D. P. (2009) Molecular Recognition of Single-Stranded RNA: Neomycin Binding to Poly(A). *FEBS Lett. 583*, 2269–2275.
39. Arya, D. P., Coffee, R. L., Jr., and Xue, L. (2004) From Triplex to B-Form Duplex Stabilization: Reversal of Target Selectivity by Aminoglycoside Dimers. *Bioorg. Med. Chem. Lett. 14*, 4643–4646.
40. Arya, D. P., Coffee, R. L., Jr., and Willis, A., III (2001) Triple Helix Stabilization by Aminoglycoside Antibiotics. Abstracts of Papers, 221st National Meeting of the American Chemical Society, San Francisco, CARB-088.
41. Arya, D. P., and Coffee, R. L., Jr. (2000) DNA Triple Helix Stabilization by Aminoglycoside Antibiotics. *Bioorg. Med. Chem. Lett. 10*, 1897–1899.
42. Arya, D. P., Shaw, N., and Xi, H. (2007) Novel Targets for Aminoglycosides. In Aminoglycoside Antibiotics: From chemical biology to drug discovery (Arya, D. P., Ed.) pp 289−314, Wiley, New York.
43. Xi, H., and Arya, D. P. (2005) Recognition of Triple Helical Nucleic Acids by Aminoglycosides. *Curr. Med. Chem. Anticancer Agents 5*, 327–338.
44. Arya, D. P., Xue, L., and Tennant, P. (2003) Combining the Best in Triplex Recognition: Synthesis and Nucleic Acid Binding of a BQQ-Neomycin Conjugate. *J. Am. Chem. Soc. 125*, 8070–8071.
45. Xue, L., Charles, I., and Arya, D. P. (2002) Pyrene-Neomycin Conjugate: Dual Recognition of a DNA Triple Helix. *Chem. Commun. 1*, 70–71.
46. Doyle, M. L., Brigham-Burke, M., Blackburn, M. N., Brooks, I. S., Smith, T. M., Newman, R., Reff, M., Stafford, W. F., Sweet, R. W., Truneh, A., Hensley, P., and O'Shannessy, D. J. (2000) Measurement of Protein Interaction Bioenergetics: Application to Structural Variants of Anti-sCD4 Antibody. *Methods Enzymol. 323*, 207–230.
47. Ren, J., and Chaires, J. B. (2001) Rapid Screening of Structurally Selective Ligand Binding to Nucleic Acids. *Methods Enzymol. 340*, 99–108.
48. Kirk, S. R., Luedtke, N. W., and Tor, Y. (2000) Neomycin-Acridine Conjugate: A Potent Inhibitor of Rev-RRE Binding. *J. Am. Chem. Soc. 122*, 980–981.
49. Arya, D. P., Xue, L., and Willis, B. (2003) Aminoglycoside (Neomycin) Preference is for A-Form Nucleic Acids, Not just RNA: Results from a Competition Dialysis Study. *J. Am. Chem. Soc. 125*, 10148–10149.
50. Charles, I., and Arya, D. P. (2005) Synthesis of Neomycin-DNA/peptide Nucleic Acid Conjugates. *J. Carbohydr. Chem. 24*, 145–160.
51. Boger, D. L., Fink, B. E., Brunette, S. R., Tse, W. C., and Hedrick, M. P. (2001) A Simple, High-Resolution Method for Establishing DNA Binding Affinity and Sequence Selectivity. *J. Am. Chem. Soc. 123*, 5878–5891.
52. Boger, D. L., and Tse, W. C. (2001) Thiazole Orange as the Fluorescent Intercalator in a High Resolution Fid Assay for Determining DNA Binding Affinity and Sequence Selectivity of Small Molecules. *Bioorg. Med. Chem. 9*, 2511–2518.
53. Escude, C., Nguyen, C. H., Kukreti, S., Janin, Y., Sun, J.-S., Bisagni, E., Garestier, T., and Helene, C. (1998) Rational Design of a Triple Helix-Specific Intercalating Ligand. *Proc. Natl. Acad. Sci. U.S.A. 95*, 3591–3596.
54. Ren, J., and Chaires, J. B. (1999) Sequence and Structural Selectivity of Nucleic Acid Binding Ligands. *Biochemistry 38*, 16067–16075.
55. McGhee, J. D. (1976) Theoretical Calculations of the Helix-Coil Transition of DNA in the Presence of Large, Cooperatively Binding Ligands. *Biopolymers 15*, 1345–1375.
56. Barbieri, C. M., and Pilch, D. S. (2006) Complete Thermodynamic Characterization of the Multiple Protonation Equilibria of the Aminoglycoside Antibiotic Paromomycin: A Calorimetric and Natural Abundance ^{15}N NMR Study. *Biophys. J. 90*, 1338–1349.